中華民國力學學會第三十屆全國力學會議　彰化縣大葉大學機械與自動化工程學系　95年12月15-16日
The 30th National Conference on Theoretical and Applied Mechanics, December 15-16, 2006, DYU, Changhwa, Taiwan, R.O.C.

Null-field Approach for Boundary Value Problems with Circular Inclusions

An-Chien Wu and Jeng-Tzong Chen

Department of Harbor and River Engineering
National Taiwan Ocean University
M93520008@mail.ntou.edu.tw

NSC PROJECT: NSC 95-2115-M-019-003-MY2

ABSTRACT

In this study, the boundary value problem with circular inclusions is formulated by using the null-field integral equation. To fully capture circular geometries, separable expressions of fundamental solutions in the polar coordinate for field and source points and Fourier series for boundary densities are introduced to derive the formulation analytically. Intermediate advantages are obtained: (1) well-posed model, (2) singularity free, (3) boundary-layer effect free, (4) exponential convergence and (5) mesh free. The method is basically a numerical approach, and because of its semi-analytical nature, it possesses certain advantages over the conventional boundary element method. The null-field approach employing the degenerate kernel and Fourier expansion can be applied to solve boundary value problems which are governed by the Laplace, Helmholtz, biharmonic and biHelmholtz equations. Problems for the anti-plane elasticity as well as the in-plane electrostatic and anti-plane piezoelectricity study are revisited to demonstrate the validity of our method.

Keywords: null-field approach, degenerate kernel, Fourier series, boundary value problem, boundary-layer effect, circular boundary.

1. INTRODUCTION

Engineering analysis can be formulated as mathematical models of boundary value problems. In order to solve the boundary value problems, researchers and engineers have paid more attention on the development of boundary integral equation method (BIEM), boundary element method (BEM) and meshless method than domain type methods, finite element method (FEM) and finite difference method (FDM). Among various numerical methods, BEM is one of the most popular numerical approaches for solving boundary value problems. Although BEM has been involved as an alternative numerical method for solving engineering problems, five critical issues are of concern.

(1) Treatment of singularity and hypersingularity

It is well known that BEM are based on the use of fundamental solutions to solve partial differential equations. These solutions are two-point functions which are singular as the source and field points coincide. Most of the efforts have been focused on the singular boundary integral equation for problems with ordinary boundaries. In some situations, the singular boundary integral equation is not sufficient, *e.g.* degenerate boundary, fictitious frequency and spurious eigenvalue. Therefore, the hypersingular equation is required. The role of hypersingularity in computational mechanics has been examined in the review article of Chen and Hong [4]. In the past, several regularizations for hypersingularity were offered to handle it in direct and indirect ways.

(2) Boundary-layer effect

Boundary-layer effect in BEM has received attention in the recent years. In real applications, data near the boundary can be smoothened since the maximum principle always exists for potential problems. Nevertheless, it also deserves study to know how to manipulate the nearly singular integrals in applied mathematics.

(3) Convergence rate

Undoubtedly, BEM is very popular for boundary value problems with general geometries since it requires discretization on the boundary only. Regarding to constant, linear and quadratic elements, the discretization scheme does not take the special geometry into consideration. It leads to the slow convergence rate.

(4) Ill-posed model

To avoid directly calculating the singular and hypersingular integrals by using null-field approach or fictitious BEM yields an ill-conditioned system. The influence matrix is not diagonally dominated and needs preconditioning. To approach the fictitious boundary to the real boundary or to move the null-field point to the real boundary can make the system well-posed. However, singularity appears in the meantime.

(5) Mesh generation

Mesh on the boundary is still necessary using BEM.

In this paper, we develop a semi-analytical approach for boundary value problems with circular inclusions by using the null-field integral equation in conjunction with the degenerate kernel and Fourier series. The adaptive observer system is proposed to fully employ the property of degenerate kernel. All the boundary integrals are

analytically determined through the orthogonal property between the degenerate kernel and Fourier series. Therefore, improper integrals are transformed to series sums instead of the sense of principal values. A linear algebraic equation is formulated to determine the unknown Fourier coefficients after collocating the null-field point on the boundary and matching the boundary condition. For the calculation of potential gradient, the Hadamard principal value for hypersingularity is not required and can be easily calculated by using series sums and by adapting the vector decomposition technique for eccentric cases. In addition, the boundary-layer effect for stress calculations near the boundary and the convergence test with various terms of Fourier series are studied. Engineering applications containing multiple circular holes and/or inclusions are demonstrated to see the validity of present method. The extension to study on coupling effect of electrical and mechanical loadings for piezoelectricity problems is also done in this paper.

2. A UNIFIED FORMULATION FOR EXTERIOR AND INTERIOR PROBLEMS

2.1 Dual boundary integral equations and dual null-field integral equations

Suppose there are N randomly distributed circular inclusions bounded to the contours B_k ($k = 0, 1, 2, \cdots, N$). We define

$$B = \bigcup_{k=0}^{N} B_k \,. \tag{1}$$

In mathematical physics, many engineering problems can be modeled by the governing equation,

$$\mathcal{L}\,\varphi(\mathrm{x}) = 0, \quad \mathrm{x} \in D, \tag{2}$$

where $\mathcal{L}$ may be the Laplacian, Helmholtz, biharmonic or biHelmholtz operators, $\varphi(\mathrm{x})$ is the potential function and D is the domain of interest. For the two-dimensional second-order operators of Laplacian and Helmholtz, the boundary integral equation for the domain point can be derived from the third Green's identity [4], we have

$$2\pi\varphi(\mathrm{x}) = \int_B T(\mathrm{s},\mathrm{x})\varphi(\mathrm{s})dB(\mathrm{s}) - \int_B U(\mathrm{s},\mathrm{x})\psi(\mathrm{s})dB(\mathrm{s}), \quad \mathrm{x} \in D, \tag{3}$$

$$2\pi\frac{\partial\varphi(\mathrm{x})}{\partial \mathrm{n}_\mathrm{x}} = \int_B M(\mathrm{s},\mathrm{x})\varphi(\mathrm{s})dB(\mathrm{s}) - \int_B L(\mathrm{s},\mathrm{x})\psi(\mathrm{s})dB(\mathrm{s}), \quad \mathrm{x} \in D, \tag{4}$$

where s and x are the source and field points, respectively, $\psi(\mathrm{s}) = \partial\varphi(\mathrm{s})/\partial \mathrm{n}_\mathrm{s}$, B is the boundary, n_x denotes the outward normal vector at the field point x and the kernel function $U(\mathrm{s},\mathrm{x})$ is the fundamental solution which satisfies

$$\mathcal{L}\,U(\mathrm{s},\mathrm{x}) = 2\pi\delta(\mathrm{x}-\mathrm{s}), \tag{5}$$

in which $\delta(\mathrm{x}-\mathrm{s})$ denotes the Dirac-delta function. The other kernel functions, $T(\mathrm{s},\mathrm{x})$, $L(\mathrm{s},\mathrm{x})$ and $M(\mathrm{s},\mathrm{x})$, are defined by

$$T(\mathrm{s},\mathrm{x}) \equiv \frac{\partial U(\mathrm{s},\mathrm{x})}{\partial \mathrm{n}_\mathrm{s}}, \; L(\mathrm{s},\mathrm{x}) \equiv \frac{\partial U(\mathrm{s},\mathrm{x})}{\partial \mathrm{n}_\mathrm{x}}, \quad M(\mathrm{s},\mathrm{x}) \equiv \frac{\partial^2 U(\mathrm{s},\mathrm{x})}{\partial \mathrm{n}_\mathrm{s}\,\partial \mathrm{n}_\mathrm{x}}, \tag{6}$$

where n_s is the outward normal vector at the source point s. By moving the field point to the boundary, Eqs. (3) and (4) reduce to

$$\pi\varphi(\mathrm{x}) = C.P.V.\int_B T(\mathrm{s},\mathrm{x})\varphi(\mathrm{s})dB(\mathrm{s}) - R.P.V.\int_B U(\mathrm{s},\mathrm{x})\psi(\mathrm{s})dB(\mathrm{s}), \quad \mathrm{x} \in B, \tag{7}$$

$$\pi\frac{\partial\varphi(\mathrm{x})}{\partial \mathrm{n}_\mathrm{x}} = H.P.V.\int_B M(\mathrm{s},\mathrm{x})\varphi(\mathrm{s})dB(\mathrm{s}) - C.P.V.\int_B L(\mathrm{s},\mathrm{x})\psi(\mathrm{s})dB(\mathrm{s}), \quad \mathrm{x} \in B, \tag{8}$$

where $C.P.V.$, $R.P.V.$ and $H.P.V.$ denote the Cauchy principal value, Riemann principal value and Hadamard principal value, respectively. Once the field point x locates outside the domain, the null-field integral equation of the direct method in Eqs. (7) and (8) yield

$$0 = \int_B T(\mathrm{s},\mathrm{x})\varphi(\mathrm{s})dB(\mathrm{s}) - \int_B U(\mathrm{s},\mathrm{x})\psi(\mathrm{s})dB(\mathrm{s}), \quad \mathrm{x} \in D^c, \tag{9}$$

$$0 = \int_B M(\mathrm{s},\mathrm{x})\varphi(\mathrm{s})dB(\mathrm{s}) - \int_B L(\mathrm{s},\mathrm{x})\psi(\mathrm{s})dB(\mathrm{s}), \quad \mathrm{x} \in D^c, \tag{10}$$

where D^c is the complementary domain. Note that the conventional null-field integral equations are not singular since s and x never coincide. If the kernel function in Eqs. (3), (4), (9) and (10) can be described as degenerate (separate) forms for the inside D or outside D^c domain, we have

$$2\pi\varphi(\mathrm{x}) = \int_B T(\mathrm{s},\mathrm{x})\varphi(\mathrm{s})dB(\mathrm{s}) - \int_B U(\mathrm{s},\mathrm{x})\psi(\mathrm{s})dB(\mathrm{s}), \quad \mathrm{x} \in D \cup B, \tag{11}$$

$$2\pi\frac{\partial\varphi(\mathrm{x})}{\partial \mathrm{n}_\mathrm{x}} = \int_B M(\mathrm{s},\mathrm{x})\varphi(\mathrm{s})dB(\mathrm{s}) - \int_B L(\mathrm{s},\mathrm{x})\psi(\mathrm{s})dB(\mathrm{s}), \quad \mathrm{x} \in D \cup B, \tag{12}$$

$$0 = \int_B T(\mathrm{s},\mathrm{x})\varphi(\mathrm{s})dB(\mathrm{s}) - \int_B U(\mathrm{s},\mathrm{x})\psi(\mathrm{s})dB(\mathrm{s}), \quad \mathrm{x} \in D^c \cup B, \tag{13}$$

$$0=\int_B M(\mathrm{s},\mathrm{x})\varphi(\mathrm{s})dB(\mathrm{s}) - \int_B L(\mathrm{s},\mathrm{x})\psi(\mathrm{s})dB(\mathrm{s}),\ \mathrm{x}\in D^c\cup B. \tag{14}$$

It is noted that the boundary integral equation for the domain point and the null-field integral equation for the null-field point can include the collocation point exactly on the real boundary since the appropriate kernel can be used as elaborated on later in the following section.

2.2 Expansions of fundamental solution and boundary density

Now, we adopt the mathematical tools, degenerate kernels and Fourier series, for the purpose of analytical study. The combination of degenerate kernels and Fourier series plays the major role in handling problems with circular boundaries. Instead of directly calculating the *C.P.V.*, *R.P.V.* and *H.P.V.* in Eqs. (7) and (8), we obtain the linear algebraic system from the null-field integral equation of Eqs. (13) and (14) through the kernel expansion by "exactly" collocating the point on the real boundary. Based on the separable property, the kernel function $U(\mathrm{s},\mathrm{x})$ can be expanded into the separable form by dividing the source and field points:

$$U(\mathrm{s},\mathrm{x})=\begin{cases} U^i(\mathrm{s},\mathrm{x})=\sum_j A_j(\mathrm{s})B_j(\mathrm{x}),\ |\mathrm{s}|\geq|\mathrm{x}| \\ U^e(\mathrm{s},\mathrm{x})=\sum_j A_j(\mathrm{x})B_j(\mathrm{s}),\ |\mathrm{x}|>|\mathrm{s}| \end{cases}, \tag{15}$$

where the bases of $A(\cdot)$ and $B(\cdot)$ can be found for the Laplacian, Helmholtz, biharmonic and biHelmholtz operators and the superscripts "i" and "e" denote the interior ($|\mathrm{s}|>|\mathrm{x}|$) and exterior ($|\mathrm{x}|>|\mathrm{s}|$) cases, respectively. For the degenerate form of T, L and M kernels, they can be derived according to their definitions in Eq. (6). Regarding the multiply-connected domain problems, the interior "i" and exterior "e" expansions for the kernel should be taken with care. Although the mathematical tools of degenerate kernels, are suitable for the Laplacian, Helmholtz, biharmonic and biHelmholtz operators in one, two and three dimensional problems, we focus on the two-dimensional Laplace problems in this papr. Based on the separable property, the kernel function $U(\mathrm{s},\mathrm{x})=\ln r$, ($r\equiv|\mathrm{x}-\mathrm{s}|$), is expanded into the degenerate form by separating the source point and field point in the polar coordinate [3]:

$$U(\mathrm{s},\mathrm{x})=\begin{cases} U^i(R,\theta;\rho,\phi)=\ln R \\ \qquad -\sum_{m=1}^{\infty}\frac{1}{m}(\frac{\rho}{R})^m\cos m(\theta-\phi),\ R\geq\rho \\ U^e(R,\theta;\rho,\phi)=\ln\rho \\ \qquad -\sum_{m=1}^{\infty}\frac{1}{m}(\frac{R}{\rho})^m\cos m(\theta-\phi),\ \rho>R \end{cases}, \tag{16}$$

where the superscripts "i" and "e" denote the interior ($R>\rho$) and exterior ($\rho>R$) cases, respectively. The origin of the observer system for the degenerate kernel is (0,0). It is noted that the leading term and numerator term in Eq. (16) involve the larger argument to ensure the log singularity and series convergence, respectively.

For problems with circular boundaries, we apply the Fourier series expansions to approximate the potential φ and its normal derivative ψ on the boundary B_k as

$$\varphi(\mathrm{s}_k)=a_0^k+\sum_{n=1}^{L}(a_n^k\cos n\theta_k+b_n^k\sin n\theta_k),\quad \mathrm{s}_k\in B_k,\ k=0,1,2,\cdots,N, \tag{17}$$

$$\psi(\mathrm{s}_k)=p_0^k+\sum_{n=1}^{L}(p_n^k\cos n\theta_k+q_n^k\sin n\theta_k),\quad \mathrm{s}_k\in B_k,\ k=0,1,2,\cdots,N, \tag{18}$$

where $\psi(\mathrm{s}_k)=\partial\varphi(\mathrm{s}_k)/\partial\mathrm{n}_\mathrm{s}$, a_n^k, b_n^k, p_n^k and q_n^k ($n=0,1,2,\cdots,L$) are the Fourier coefficients and θ_k is the polar angle. In the real computation, only $2L+1$ finite terms are considered where L indicates the truncated terms of Fourier series.

2.3 Adaptive observer system

By using the collocation method, the null-field integral equation becomes a set of algebraic equations for the Fourier coefficients. To ensure the stability of algebraic equations, one has to choose collocation points throughout all the circular boundaries. Since the boundary integral equation is derived from the reciprocal theorem of energy concept, the boundary integral equation is frame indifferent due to the objectivity rule. This is the reason why the observer system is adaptively selected to locate the origin at the center of circle in the boundary integration. The adaptive observer system is chosen to fully employ the property of degenerate kernels. Figures 1 (a) and 1 (b) show the boundary integration for the circular boundary in the adaptive observer system. It is worth noting that the origin of the observer system is located on the center of the corresponding circle under integration to entirely utilize the geometry of circular boundary for the expansion of degenerate kernels and boundary densities. The dummy variable in the circular integration is the angle (θ) instead of the radial coordinate (R).

2.4 Linear algebraic equation

By moving the null-field point x_m to the *kth* circular boundary in the limit sense for Eq. (13) in Fig. 1 (a), we have

$$0=\sum_{k=0}^{N}\int_{B_k}T(\mathrm{s}_k,\mathrm{x}_m)\varphi(\mathrm{s}_k)dB_k - \sum_{k=0}^{N}\int_{B_k}U(\mathrm{s}_k,\mathrm{x}_m)\psi(\mathrm{s}_k)dB_k,\ \mathrm{x}_m\in D^c\cup B, \tag{19}$$

where N is the number of circular inclusions and B_0 denotes the outer boundary for the bounded domain. In case of the infinite problem, B_0 becomes B_∞. Note

that the kernels $U(\mathrm{s},\mathrm{x})$ and $T(\mathrm{s},\mathrm{x})$ are shown in the degenerate form and the boundary densities φ and ψ are expressed in terms of the Fourier series expansion forms as mention above. Then, the integrals multiplied by separate expansion coefficients in Eq. (19) are non-singular and the limit of the null-field point to the boundary is easily implemented by using appropriate forms of degenerate kernels. Through such an idea, all the singular and hypersingular integrals are well captured. Thus, the collocation point x_m in the discretized Eq. (19) can be considered on the boundary B_k, as well as the null-field point. Along each circular boundary, $2L+1$ collocation points are required to match $2L+1$ terms of Fourier series for constructing a square influence matrix with the dimension of $2L+1$ by $2L+1$. In contrast to the standard discretized boundary integral equation formulation with nodal unknowns of the physical boundary densities φ and ψ, now the degrees of freedom are transformed to Fourier coefficients employed in expansion of boundary densities. It is found that the compatible relationship of the boundary unknowns is equivalent by moving either the null-field point or the domain point to the boundary in different directions using various degenerate kernels as shown in Figs. 1 (a) and 1 (b). Both approaches yield the same linear algebraic equation due to the Wronskian property [14]. In the B_k integration, we set the origin of the observer system to collocate at the center c_k to fully utilize the degenerate kernels and Fourier series. By collocating the null-field point on the boundary, the linear algebraic system is obtained

$$[\mathbf{U}]\{\psi\}=[\mathbf{T}]\{\varphi\}, \tag{20}$$

where $[\mathbf{U}]$ and $[\mathbf{T}]$ are the influence matrices with a dimension of $(N+1)(2L+1)$ by $(N+1)(2L+1)$, $\{\varphi\}$ and $\{\psi\}$ denote the column vectors of Fourier coefficients with a dimension of $(N+1)(2L+1)$ by 1 in which those are defined as follows:

$$[\mathbf{U}]=\begin{bmatrix}\mathbf{U}_{00} & \mathbf{U}_{01} & \cdots & \mathbf{U}_{0N}\\ \mathbf{U}_{10} & \mathbf{U}_{11} & \cdots & \mathbf{U}_{1N}\\ \vdots & \vdots & \ddots & \vdots\\ \mathbf{U}_{N0} & \mathbf{U}_{N1} & \cdots & \mathbf{U}_{NN}\end{bmatrix},\ \{\varphi\}=\begin{Bmatrix}\varphi_0\\ \varphi_1\\ \varphi_2\\ \vdots\\ \varphi_N\end{Bmatrix}, \tag{21}$$

$$[\mathbf{T}]=\begin{bmatrix}\mathbf{T}_{00} & \mathbf{T}_{01} & \cdots & \mathbf{T}_{0N}\\ \mathbf{T}_{10} & \mathbf{T}_{11} & \cdots & \mathbf{T}_{1N}\\ \vdots & \vdots & \ddots & \vdots\\ \mathbf{T}_{N0} & \mathbf{T}_{N1} & \cdots & \mathbf{T}_{NN}\end{bmatrix},\ \{\psi\}=\begin{Bmatrix}\psi_0\\ \psi_1\\ \psi_2\\ \vdots\\ \psi_N\end{Bmatrix}, \tag{22}$$

where $\{\varphi_k\}$ and $\{\psi_k\}$ are in the form of Fourier coefficients given by Eqs. (17) and (18), respectively; the first subscript "j" ($j=0,1,2,\cdots,N$) in $[\mathbf{U}_{jk}]$ and $[\mathbf{T}_{jk}]$ denotes the index of the *jth* circle where the collocation point is located and the second subscript "k" ($k=0,1,2,\cdots,N$) denotes the index of the *kth* circle when integrating on each boundary data $\{\varphi_k\}$ and $\{\psi_k\}$, N is the number of circular inclusions in the domain and the number L indicates the truncated terms of Fourier series. The coefficient matrix of the linear algebraic system is partitioned into blocks, and each off-diagonal block corresponds to the influence matrices between two different circular boundaries. The diagonal blocks are the influence matrices due to themselves in each individual circle. Instead of using nodal values for boundary densities in the BEM, the Fourier coefficients become the new unknown degrees of freedom in the formulation.

Regarding the circular inclusion problems in the infinite domain, it can be decomposed to one exterior and several interior Laplace problems with circular boundaries after taking free body along the interface of matrix and each inclusion. Two kinds of problems can be formulated in a unified manner as shown in Eq. (20) after superimposing remote loadings:

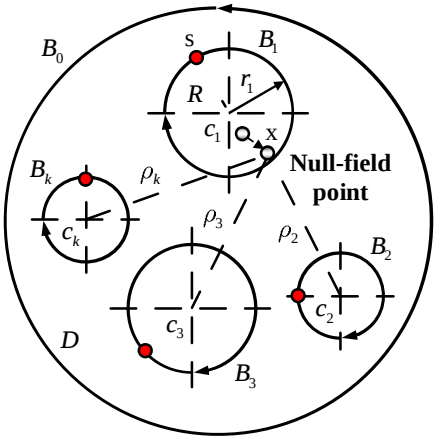

Figure 1 (a) Sketch of the null-field integral equation for a null-field point in conjunction with the adaptive observer system ($\mathrm{x}\notin D$, $\mathrm{x}\to B_k$)

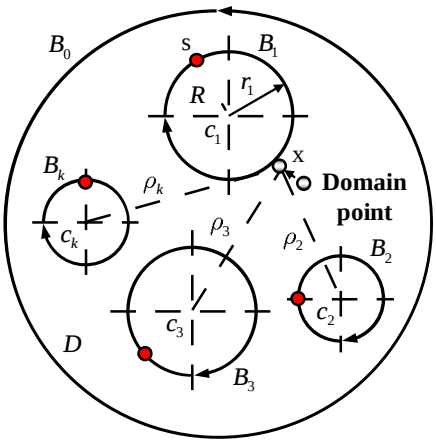

Figure 1 (b) Sketch of the boundary integral equation for a domain point in conjunction with the adaptive observer system ($\mathrm{x}\in D$, $\mathrm{x}\to B_k$)

(1) One bounded problem of the circular domain becomes the interior problem for each inclusion as the only boundary B_0 in Fig. 1 (a) exists.
(2) The other is unbounded, *i.e.* the outer boundary B_0 in Fig. 1 (a) is B_∞. It is the exterior problem for the matrix.

The direction of contour integration should be taken care, *i.e.* counterclockwise and clockwise directions are for the interior and exterior problems, respectively. To match the interface condition between the matrix and each inclusion, additional constraints are provided. Then the unknown Fourier coefficients can be obtained from the resulted linear algebraic system. In order to determine the field of potential gradient, the normal and tangential derivatives should be calculated with care. For the nonconcentric cases, special treatment, vector decomposition technique, for the potential gradient should be considered as the source point and field point locate on different circular boundaries.

3. ILLUSTRATIVE EXAMPLES

In order to verify the efficiency and accuracy of the present method, anti-plane elasticity, in-plane electrostatic and anti-plane piezoelectricity problems are solved. For the purpose of comparison, the applied loadings and material properties of the matrix and inclusions are assumed as the same of Steif [12], Chao and Young [2], Emets and Onofrichuk [10], Pak [11] and Chao and Chang [1]. The problem statements for the three problems governed by the Laplace equation can be found in the authors' previous works [7, 8, 14].

Anti-plane elasticity problem

Figure 2 (a) shows the geometry of two equal-sized holes in the infinite medium under the remote shear $\sigma_{zy}^{\infty} = \tau_{\infty}$. The stress concentration of the problem is illustrated in Fig. 2 (b). It indicates that the present result agrees well with the analytical solution of Steif [12] and those obtained by Chao and Young [2] even though the two holes approach each other. Figure 2 (c) shows that only few terms of Fourier series can obtain good results. However, more nodes are required by using the conventional BEM to achieve convergence. Our formulation is free of boundary-layer effect instead of appearance by using the conventional BEM when the

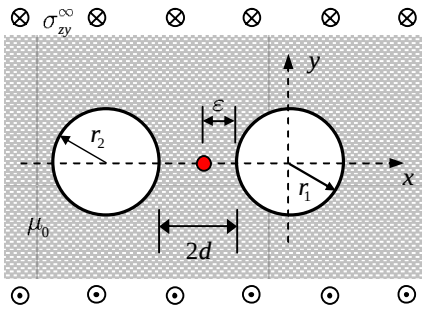

Figure 2 (a) Two equal-sized holes with centers on the x axis

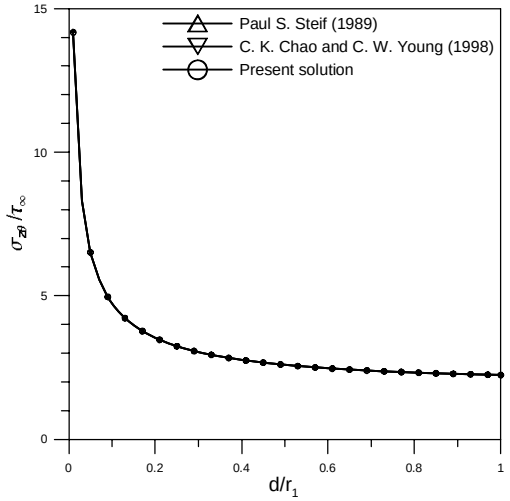

Figure 2 (b) Stress concentration of the problem containing two equal-sized holes

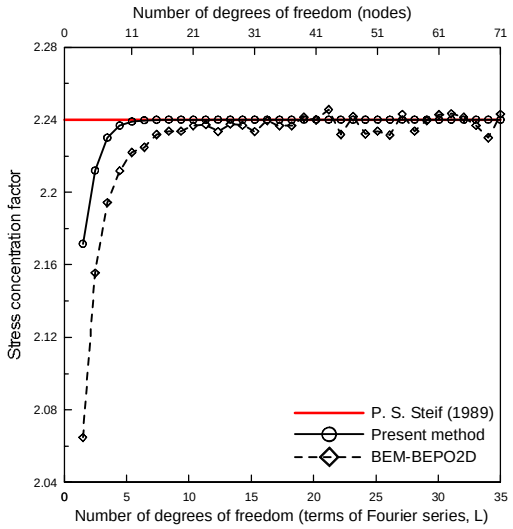

Figure 2 (c) Convergence test of the two equal-sized holes problem ($d = 1.0$)

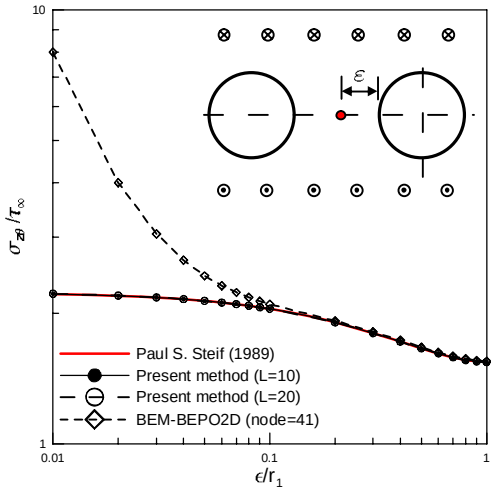

Figure 2 (d) Tangential stress in the matrix near the boundary ($d = 1.0$)

Table 1 Stress concentration factors and errors for various distances between two holes using the present approach and BEM

	d/r_1		0.01	0.2	0.4	0.6	0.8	1.0
Stress concentration factor	Analytical solution [12]		14.2247	3.5349	2.7667	2.4758	2.3274	2.2400
	Present method	$L=10$	10.5096 (26.12%)	3.5306 (0.12%)	2.7664 (0.01%)	2.4758 (0.00%)	2.3274 (0.00%)	2.2400 (0.00%)
		$L=20$	13.3275 (6.31%)	3.5349 (0.00%)	2.7667 (0.00%)	2.4758 (0.00%)	2.3274 (0.00%)	2.2400 (0.00%)
	BEM	$node=21$	7.2500 (49.03%)	3.4532 (2.31%)	2.738 (1.04%)	2.4639 (0.48%)	2.3168 (0.46%)	2.2366 (0.15%)
	BEPO2D	$node=41$	10.2008 (28.29%)	3.5188 (0.46%)	2.7619 (0.17%)	2.4747 (0.04%)	2.3312 (0.16%)	2.2398 (0.01%)

stress $\sigma_{z\theta}$ near the boundary as shown in Fig. 2 (d). Stress concentration factors and errors for various distances between two holes by using the present method and the conventional BEM are listed in Table 1. These results show that the present method is more accurate and efficient than those of the conventional BEM. Under the same error tolerance, the CPU time of the present method is fewer than that of the conventional BEM. Besides, it is noted that more terms of Fourier series are required to capture the singular behavior when the two holes approach each other.

In-plane electrostatic problem

Figure 3 (a) shows that two dielectric circular inclusions with radii of $r_2=0.8r_1$ imbedded in an infinite dielectric medium are in various uniform electric fields $E_x^\infty=E_\infty$ and $(E_x^\infty,\ E_y^\infty)=(E_\infty\cos 45^\circ,\ E_\infty\sin 45^\circ)$ applied at infinity, respectively. The distance between two inclusions is $d=0.1r_1$ and dielectric constants for matrix and each inclusion are $\varepsilon_0=3$, $\varepsilon_1=9$ and $\varepsilon_2=5$. Illustrations of the patterns of the electric field are shown in Figs. 3 (b) and 3 (c) for different loadings. From these patterns of the electric field, it is observed that the electric field is continuous across the interface between the matrix and inclusions and agrees well with those of Emets and Onofrichuk [10].

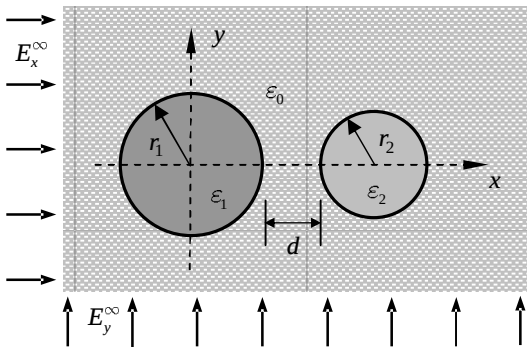

Figure 3 (a) The dielectric system of two inclusions in the applied electric field

Anti-plane piezoelectricity problem

We consider two piezoelectric circular inclusions of radii $r_2=2r_1$ perfectly bonded to a piezoelectric matrix which is subjected to the remote anti-plane shear $\sigma_{zy}^\infty=\tau_\infty$ and in-plane electric field $E_y^\infty=E_\infty$ as shown in Fig. 4 (a). In order to examine the accuracy of the present formulation, the stress concentration factor $\sigma_{z\theta}/\tau_\infty$ in the matrix at $\theta=0^\circ$ under the remote shear and the various magnitude of electric field is plotted in Fig. 4 (b) as a function of the ratio of piezoelectric constants e_{15}^M/e_{15}^I, where the two circular

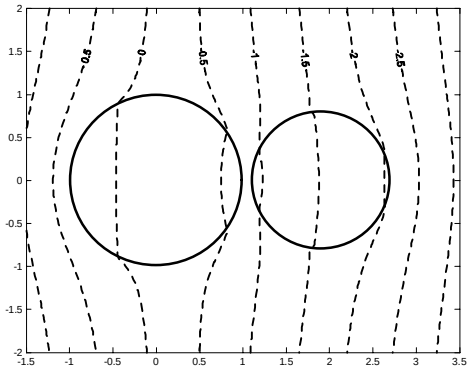

Figure 3 (b) Patterns of the electric field for $E_x^\infty=E_\infty$

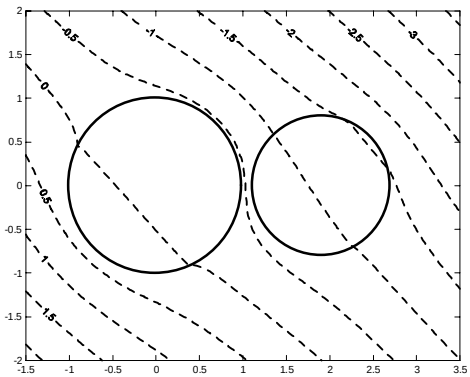

Figure 3 (c) Patterns of the electric field for $(E_x^\infty,\ E_y^\infty)=(E_\infty\cos 45^\circ,\ E_\infty\sin 45^\circ)$

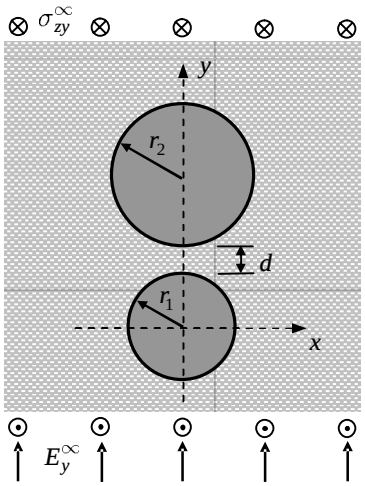

Figure 4 (a) Two piezoelectric circular inclusions embedded in a piezoelectric matrix under remote shear and electric loadings

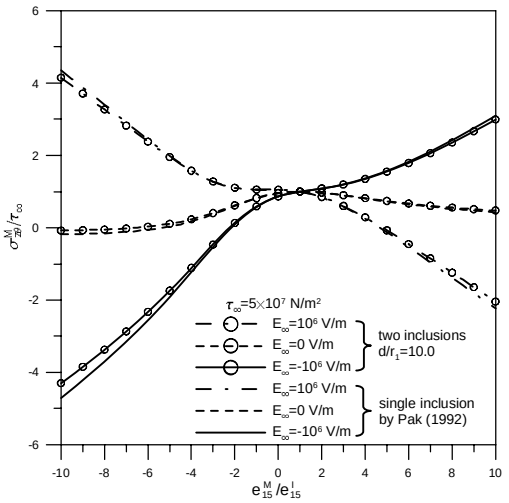

Figure 4 (b) Stress concentrations as a function of the ratio of piezoelectric constants

inclusions are arrayed parallel to the applied loadings and the distance between two circular inclusions $d/r_1 = 10$. It is found that the results displayed in Fig. 4 (b) agree very well with Chao and Chang's results [1] and approach the Pak's solution of a single inclusion [11]. The electric field concentration E_θ / E_∞ in the matrix at $\theta = 0^\circ$ with the remote electric field and the various magnitude of shear is plotted in Fig. 4 (c) as a function of the ratio of piezoelectric constants. It is also found that the results in Fig. 4 (c) leads to the Pak's solution of a single inclusion [11] since the two inclusions displace far away ($d/r_1 = 10$). The electric field concentration E_θ / E_∞ occurring at $\theta = 0^\circ$ is plotted in Fig. 4 (d) as a function of the ratio of dielectric constants $\varepsilon_{11}^M / \varepsilon_{11}^I$ while $c_{44}^M = c_{44}^I$ and $e_{15}^M = e_{15}^I$. It is shown that the electric field concentration approaches two for a large value of $\varepsilon_{11}^M / \varepsilon_{11}^I$ as $d/r_1 = 10$ which is consistent with Chao and Chang's results [1] and reduces to the Pak's solution of a single inclusion [11].

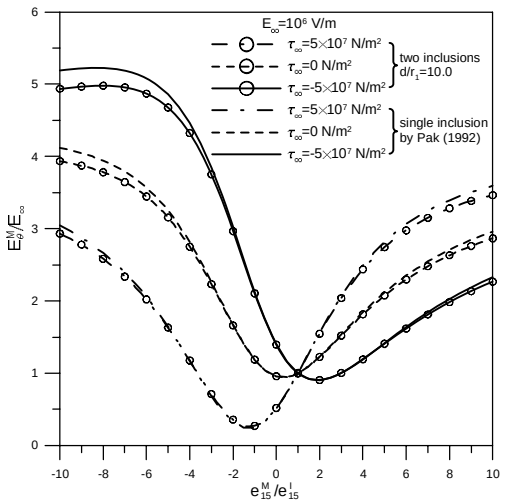

Figure 4 (c) Electric field concentrations as a function of the ratio of piezoelectric constants

4. CONCLUSION

For boundary value problems with circular inclusions, the null-field approach by using the null-field integral equation, degenerate kernels and Fourier series in the adaptive observer system was proposed. The singularity and hypersingularity were avoided after introducing the concept of degenerate kernels for interior and exterior regions. Besides, the boundary-layer effect for the potential gradient calculation was eliminated since the degenerate kernel can describe the jump behavior for interior and exterior domains, respectively. Only a few terms of Fourier series can yield acceptable results because the use of degenerate kernels for fundamental solutions and Fourier expansions for boundary densities leads to the exponential convergence. The influence matrix in the linear algebraic system using the present formulation is well-posed since the jump behavior of potential distribution was separately described in

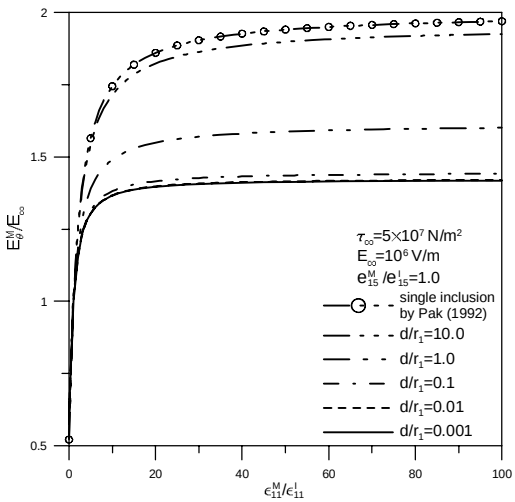

Figure 4 (d) Electric field concentrations as a function of the ratio of dielectric constants

different regions by using the degenerate kernels for the representation of fundamental solutions. Moreover, the present method here can be applied to Laplace problems with circular boundaries, *e.g.* piezoelectricity, electrostatic, magnetic, torsion, elasticity, heat conduction and hydrodynamic problems. Besides, extensions to the Helmholtz, biharmonic and biHelmholtz operators as well as 3-D problems are straightforward once the corresponding degenerate kernels and bases for boundary densities can be found. In this paper, our main demonstration is limited on the Laplace problem.

5. ACKNOWLEDGEMENT

The first author (An-Chien Wu) would like to thank the student scholarship from the China Engineering Consultants, Inc., Taiwan. This work was partially supported by the Nation al Science Council, Taiwan, through Grant NSC 95-2115-M-019-003-MY2 to National Taiwan Ocean University.

6. REFERENCES

[1] C.K. Chao and K.J. Chang, "Interacting circular inclusions in antiplane piezoelectricity," *International Journal of Solids and Structures*, vol. 36, pp. 3349-3373, 1999.

[2] C.K. Chao and C.W. Young, "On the general treatment of multiple inclusions in antiplane elastostatics," *International Journal of Solids and Structures*, vol. 35, pp. 3573-3593, 1998.

[3] J.T. Chen and Y.P. Chiu, "On the pseudo-differential operators in the dual boundary integral equations using degenerate kernels and circulants," *Engineering Analysis with Boundary Elements*, vol. 26, pp. 41-35, 2002.

[4] J.T. Chen and H.-K. Hong, "Review of dual boundary element methods with emphasis on hypersingular integrals and divergent series," *ASME Applied Mechanics Reviews*, vol. 52, pp. 17-33, 1999.

[5] J.T. Chen, C.C. Hsiao and S.Y. Leu, "Null-field integral equation approach for plate problems with circular boundaries," *ASME Journal of Applied Mechanics*, vol. 73, pp. 679-693, 2006.

[6] J.T. Chen, W.C. Shen and A.C. Wu, "Null-field integral equations for stress field around circular holes under antiplane shear," *Engineering Analysis with Boundary Elements*, vol. 30, pp. 205-217, 2006.

[7] J.T. Chen and A.C. Wu, "Null-field approach for piezoelectricity problems with arbitrary circular inclusions," *Engineering Analysis with Boundary Elements*, accepted, 2006.

[8] J.T. Chen and A.C. Wu, "Null-field approach for the multi-inclusion problem under anti-plane shears," *ASME Journal of Applied Mechanics*, accepted, 2006.

[9] T. Chen and S.C. Chiang, "Electroelastic fields and effective moduli of a medium containing cavities or rigid inclusions of arbitrary shape under anti-plane mechanical and in-plane electric fields," *Acta Mechanica*, vol. 121, pp. 79-96, 1997.

[10] Y.P. Emets and Y.P. Onofrichuk, "Interaction forces of dielectric cylinders in electric fields," *IEEE Transactions on Dielectrics and Electrical Insulation*, vol. 3, pp.87-98, 1996.

[11] Y.E. Pak, "Circular inclusion problem in antiplane piezoelectricity," *International Journal of Solids and Structures*, vol. 29, pp. 2403-2419, 1992.

[12] P.S. Steif, "Shear stress concentration between holes," *ASME Journal of Applied Mechanics*, vol. 56, pp. 719-721, 1989.

[13] X.Wang and Y.-P. Shen, "On double circular inclusion problem in antiplane piezoelectricity," *International Journal of Solids and Structures*, vol. 38, pp. 4439-4461, 2001.

[14] A.C. Wu, "Null-field approach for multiple circular inclusion problems in anti-plane piezoelectricity," Master Thesis, *Department of Harbor and River Engineering, National Taiwan Ocean University*, Keelung, Taiwan, 2006.

[15] L.Z. Wu and K. Funami, "The electro-elastic field of the infinite piezoelectric medium with two piezoelectric circular cylindrical inclusions," *Acta Mechanica Sinica*, vol. 18, pp. 368-385, 2002.

零場積分方程求解含圓形夾雜之邊界值問題

吳安傑 陳正宗

國立台灣海洋大學河海工程學系

摘要

本文係使用零場積分方程求解含圓形夾雜之邊界值問題。為了充分利用圓形邊界的特性，將基本解以場、源點分離的概念展開為分離（退化）的型式，而邊界物理量則以傅立葉級數展開，搭配自適性觀察座標系統來解析求出邊界積分；因此可以獲得五大好處：矩陣良態模式、避免奇異積分、沒有邊界層效應、指數收斂、不必建構網格。相對於傳統邊界元素法，此半解析法擁有某種程度的優越性。此利用零場積分方程搭配分離核及傅立葉級數之方法，可廣泛地用來求解拉普拉斯、赫姆茲、雙諧和、雙赫姆茲之邊界值問題。最後，為了驗證此方法的有效性，對反平面彈力問題、平面靜電場問題與反平面壓電問題均予以測試。

關鍵詞：零場積分方程、分離核函數、傅立葉級數、邊界值問題、邊界層效應、圓形邊界。